EPJ B
Condensed Matter and Complex Systems
www.epj.org

Eur. Phys. J. B **67**, 565–576 (2009) DOI: 10.1140/epjb/e2009-00058-x

# Electronic properties of double-layer carbon nanotubes

M. Pudlak and R. Pincak

EDP SCIENCES
Società Italiana di Fisica
Springer

Eur. Phys. J. B **67**, 565–576 (2009)
DOI: 10.1140/epjb/e2009-00058-x

THE EUROPEAN PHYSICAL JOURNAL B

Regular Article

# Electronic properties of double-layer carbon nanotubes

M. Pudlak[1] and R. Pincak[1,2,a]

[1] Institute of Experimental Physics, Slovak Academy of Sciences, Watsonova 47, 043 53 Kosice, Slovak Republic
[2] Joint Institute for Nuclear Research, BLTP, 141980 Dubna, Moscow region, Russia

Received 7 August 2008 / Received in final form 15 January 2009
Published online 18 February 2009 – 

**Abstract.** The electronic spectra for double-wall zigzag and armchair nanotubes are found. The influence of nanotube curvatures on the electronic spectra is also calculated. Our finding that the outer shell is hole doped by the inner shell is in the difference between Fermi levels of individual shells which originate from the different hybridization of $\pi$ orbital. The shift and rotation of the inner nanotube with respect to the outer nanotube are investigated. We found stable semimetal characteristics of the armchair DWNTs in regard of the shift and rotation of the inner nanotube. We predict the shift of $k_F$ towards the bigger wave vectors with decreasing of the radius of the armchair nanotube.

**PACS.** 73.63.-b Electronic transport in nanoscale materials and structures – 73.63.Fg Nanotubes – 73.22.-f Electronic structure of nanoscale materials: clusters, nanoparticles, nanotubes, and nanocrystals

## 1 Introduction

Carbon nanotubes are very interesting because of their unique mechanical and electronic properties. A single-wall carbon nanotube can be described as a graphene sheet rolled into a cylindrical shape so that the structure is one-dimensional with axial symmetry and in general exhibiting a spiral conformation called chirality. The primary symmetry classification of carbon nanotubes is either achiral (symmorphic) or chiral (non-symmorphic). Achiral carbon nanotubes are defined by a carbon nanotube whose mirror images have an identical structure to the original one. There are only two cases of achiral nanotubes, armchair and zigzag nanotubes. The names of armchair and zigzag nanotubes arise from the shape of the cross-section ring at the edge of the nanotubes. Chiral nanotubes exhibit spiral symmetry whose mirror image cannot be superposed onto the original one. There is a variety of geometries in carbon nanotubes which can change the diameter, chirality and cap structures. The electronic structure of carbon nanotubes is derived by a simple tight-binding calculation for the $\pi$-electrons of carbon atoms. Of special interest is the prediction that the calculated electronic structure of a carbon nanotube can be either metallic or semiconducting, depending on its diameter and chirality. The energy gap for a semiconductor nanotube, which is inversely proportional to its diameters, can be directly observed by scanning tunneling microscopy measurements. The electronic structure of a single-wall nanotube can be obtained simply from that of two-dimensional graphite. By using periodic boundary conditions in the circumferential direction denoted by the chiral vector $C_h$, the wave vector associated with the $C_h$ direction becomes quantized, while the wave vector associated with the direction of the translational vector $T$ along the nanotube axis remains continuous for a nanotube of infinite length. Thus, the energy bands consist of a set of one-dimensional energy dispersion relations which are cross sections of those for two-dimensional graphite. To obtain explicit expressions for the dispersion relations, the simplest cases to consider are the nanotubes having the highest symmetry, e.g. highly symmetric achiral nanotubes. The synthesis of DWNTs has been reported recently [1,2]. Their electronic structure was investigated by the local density approximation [3–7] and the tight-binding model [8–11]. A similar method can be used to investigate the electronic spectra of the fullerene molecules [12,13]. In this paper we are interested in the zigzag and armchair double-wall nanotubes (DWNTs) with a small radius. In these DWNTs the difference of Fermi levels of individual nanotubes has to be taken into account. We focus on $(9,0)$–$(18,0)$ zigzag tubules and $(5,5)$–$(10,10)$ armchair tubules. They are the best matched, double layer tubules.

## 2 (9, 0)–(18, 0) zigzag tubules

Firstly, we describe the model for the zigzag nanotubes. The $\pi$ electronic structures are calculated from the

[a] e-mail: pincak@saske.sk

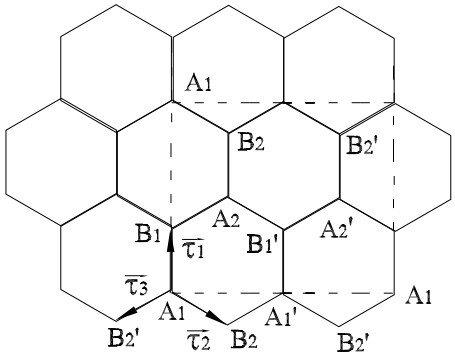


**Fig. 1.** The outer shell part of the unit cell in the case of zigzag nanotubes.

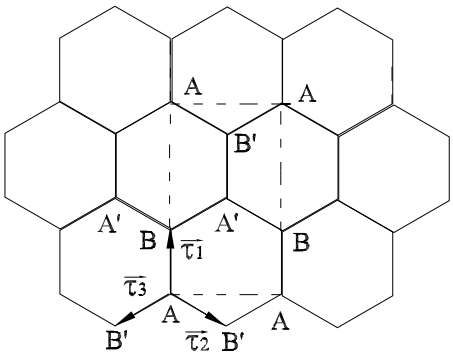


**Fig. 2.** The inner shell part of the unit cell in the case of zigzag nanotubes.

tight-binding Hamiltonian

$$H = \sum_i \epsilon|\varphi_i^{out}\rangle\langle\varphi_i^{out}| + \sum_{i,j}\gamma_{ij}\left(|\varphi_i^{in}\rangle\langle\varphi_j^{in}| + h.c\right) + \sum_i \widetilde{\epsilon}|\varphi_i^{in}\rangle\langle\varphi_i^{in}| + \sum_{i,j}\widetilde{\gamma}_{ij}\left(|\varphi_i^{in}\rangle\langle\varphi_j^{in}| + h.c\right) + \sum_{l,n} W_{ln}\left(|\varphi_l^{in}\rangle\langle\varphi_n^{out}| + h.c\right), \quad (1)$$

$\epsilon$ and $\widetilde{\epsilon}$ are Fermi energies of the outer and inner nanotubes; $|\varphi_i^{out}\rangle$, $|\varphi_i^{in}\rangle$ are $\pi$ orbitals on site $i$ at the outer and inner tubes; $\gamma_{ij}$, $\widetilde{\gamma}_{ij}$ are the intratube hopping integrals; $W_{ij}$ are the intertube hoping integrals which depends on the distance $d_{ij}$ and angle $\theta_{ij}$ between the $\pi_i$ and $\pi_j$ orbitals (see [14–16] for details).

$$W_{ij} = \frac{\gamma_0}{8}\cos(\theta_{ij})e^{(\xi - d_{ij})/\delta}, \quad (2)$$

where $\theta_{ij}$ is an angle between the $i$th atom of the inner shell and the $j$th atom of the outer shell, $d_{ij}$ is the interatom distance and $\xi$ is a intertube distance. The characteristic length $\delta = 0.45$ Å.

To describe the parameter which characterized the zigzag tubules, we start from the graphene layer [17] where we can define the vectors connecting the nearest neighbor carbon atoms for zigzag nanotubes in the form:

$$\overrightarrow{\tau_1} = a(0; \frac{1}{\sqrt{3}}),$$
$$\overrightarrow{\tau_2} = a(\frac{1}{2}; -\frac{1}{2\sqrt{3}}),$$
$$\overrightarrow{\tau_3} = a(-\frac{1}{2}; -\frac{1}{2\sqrt{3}}). \quad (3)$$

The distance between atoms in the unit cell is $d = |\overrightarrow{\tau_i}| = \frac{a}{\sqrt{3}}$. Following the scheme in Figures 1, 2 [18] we want to find solution to the double-layer graphene tubules in the form:

$$\psi(\overrightarrow{r}) = \psi_{out}(\overrightarrow{r}) + \psi_{in}(\overrightarrow{r}), \quad (4)$$

where

$$\psi_{out}(\overrightarrow{r}) = C_{A_1}\psi_{A_1} + C_{A_2}\psi_{A_2} + C_{B_1}\psi_{B_1} + C_{B_2}\psi_{B_2} + C_{A_1'}\psi_{A_1'} + C_{A_2'}\psi_{A_2'} + C_{B_1'}\psi_{B_1'} + C_{B_2'}\psi_{B_2'}, \quad (5)$$

and

$$\psi_{in}(\overrightarrow{r}) = C_A\psi_A + C_B\psi_B + C_{A'}\psi_{A'} + C_{B'}\psi_{B'}. \quad (6)$$

We want to find solution to the above equation in the form of the Bloch function

$$\psi_\alpha(\overrightarrow{k}, \overrightarrow{r}) = \frac{1}{\sqrt{M}}\sum_n e^{i\overrightarrow{k}(\overrightarrow{r_n} + \overrightarrow{d}_\alpha)}|\varphi(\overrightarrow{r} - \overrightarrow{r}_n - \overrightarrow{d}_\alpha)\rangle, \quad (7)$$

where $\alpha$ denotes $A$ or $B$ atoms. Here $\overrightarrow{d}_\alpha$ is the coordinate of the $\alpha$ atom in the unit cell and $\overrightarrow{r_n}$ is a position of a unit cell, $M$ is a number of the unit cell; $|\varphi(\boldsymbol{r})\rangle$ is a $\pi$ orbital which is generally different for the outer and inner shell. We denote

$$\epsilon = \langle\varphi^{out}(r - A_i)|H|\varphi^{out}(r - A_i)\rangle = \langle\varphi^{out}(r - B_i)|H|\varphi^{out}(r - B_i)\rangle, \quad (8)$$

$$\widetilde{\epsilon} = \langle\varphi^{in}(r - A_i)|H|\varphi^{in}(r - A_i)\rangle = \langle\varphi^{in}(r - B_i)|H|\varphi^{in}(r - B_i)\rangle. \quad (9)$$

Now we define the intratube hopping integrals

$$\langle\varphi^{out}(r - A_1)|H|\varphi^{out}(r - B_1)\rangle = \gamma_0,$$

$$\langle\varphi^{out}(r - A_1)|H|\varphi^{out}(r - B_2)\rangle = \gamma_0\beta = \langle\varphi^{out}(r - A_1)|H|\varphi^{out}(r - B_2')\rangle, \quad (10)$$

and

$$\langle\varphi^{in}(r - A)|H|\varphi^{in}(r - B)\rangle = \gamma_0,$$
$$\langle\varphi^{in}(r - A)|H|\varphi^{in}(r - B')\rangle = \gamma_0\widetilde{\beta}, \quad (11)$$

where $\gamma_0$ is the hoping integral in the graphene and $\beta(\widetilde{\beta})$ is part which depends on the surface curvature and will be computed latter. So in a tight-binding approximation we get the systems of equations as showing in Appendix A.

Firstly, we solve the equations in Appendix A assuming that $W_{ij}$ is the perturbation. So we can decouple these 12 equations. We get 8 equations for the outer shell and 4 for the inner shell. If we express the

state of the outer shell (Eq. (5)) in the form $\psi_{out} = (C_{A_1}, C_{B_1}, C_{A_2}, C_{B_2}, C_{A_1'}, C_{B_1'}, C_{A_2'}, C_{B_2'})$, we get the solutions to the outer shell in the form

$$E_{1,2}(k) = \epsilon \pm \gamma_0 \left(1 + 4\beta \cos\frac{m\pi}{N} \cos\frac{\sqrt{3}ka}{2} + 4\beta^2 \cos^2\frac{m\pi}{N}\right)^{\frac{1}{2}},$$
$$\psi_{1,2} = \frac{1}{\sqrt{8}} \left(1; \pm e^{-i\varphi_1}; 1; \pm e^{-i\varphi_1}, 1; \pm e^{-i\varphi_1}; 1; \pm e^{-i\varphi_1}\right) \tag{12}$$

$$E_{3,4}(k) = \epsilon \pm \gamma_0 \left(1 - 4\beta \cos\frac{m\pi}{N} \cos\frac{\sqrt{3}ka}{2} + 4\beta^2 \cos^2\frac{m\pi}{N}\right)^{\frac{1}{2}},$$
$$\psi_{3,4} = \frac{1}{\sqrt{8}} \left(1; \pm e^{-i\varphi_2}; -1; \mp e^{-i\varphi_2}, 1; \pm e^{-i\varphi_2}; -1; \mp e^{-i\varphi_2}\right) \tag{13}$$

$$E_{5,6}(k) = \epsilon \pm \gamma_0 \left(1 + 4\beta \sin\frac{m\pi}{N} \cos\frac{\sqrt{3}ka}{2} + 4\beta^2 \sin^2\frac{m\pi}{N}\right)^{\frac{1}{2}},$$
$$\psi_{5,6} = \frac{1}{\sqrt{8}} \left(1; \pm e^{-i\varphi_3}; -i; \mp ie^{-i\varphi_3}, -1; \mp e^{-i\varphi_3}; i; \pm ie^{-i\varphi_3}\right) \tag{14}$$

$$E_{7,8}(k) = \epsilon \pm \gamma_0 \left(1 - 4\beta \sin\frac{m\pi}{N} \cos\frac{\sqrt{3}ka}{2} + 4\beta^2 \sin^2\frac{m\pi}{N}\right)^{\frac{1}{2}},$$
$$\psi_{7,8} = \frac{1}{\sqrt{8}} \left(1; \pm e^{-i\varphi_4}; i; \pm ie^{-i\varphi_4}, -1; \mp e^{-i\varphi_4}; -i; \mp ie^{-i\varphi_4}\right) \tag{15}$$

where, for instance,

$$e^{i\varphi_1} = \frac{e^{i\frac{ka}{\sqrt{3}}} + 2\beta \cos\frac{m\pi}{N} e^{-i\frac{ka}{2\sqrt{3}}}}{(1 + 4\beta \cos\frac{m\pi}{N} \cos\frac{\sqrt{3}ka}{2} + 4\beta^2 \cos^2\frac{m\pi}{N})^{\frac{1}{2}}}. \tag{16}$$

Similar results for the electronic spectra in the case of inner nanotubes were found in the form ($\psi_{in} = (C_A, C_B, C_{A'}, C_{B'})$)

$$E_{9,10}(k) = \tilde{\epsilon} \pm \gamma_0 \left(1 + 4\widetilde{\beta} \cos\frac{m\pi}{N} \cos\frac{\sqrt{3}ka}{2} + 4\widetilde{\beta}^2 \cos^2\frac{m\pi}{N}\right)^{\frac{1}{2}},$$
$$\psi_{9,10} = \frac{1}{\sqrt{4}} \left(1; \pm e^{-i\varphi_5}; 1; \pm e^{-i\varphi_5}\right) \tag{17}$$

$$E_{11,12}(k) = \tilde{\epsilon} \pm \gamma_0 \left(1 - 4\widetilde{\beta} \cos\frac{m\pi}{N} \cos\frac{\sqrt{3}ka}{2} + 4\widetilde{\beta}^2 \cos^2\frac{m\pi}{N}\right)^{\frac{1}{2}},$$
$$\psi_{11,12} = \frac{1}{\sqrt{4}} \left(1; \pm e^{-i\varphi_6}; -1; \mp e^{-i\varphi_6}\right). \tag{18}$$

Since the radii of the outer and inner nanotubes are different $\beta \neq \widetilde{\beta}$. Here $k_y = k$ and $-\frac{\pi}{\sqrt{3}a} < k < \frac{\pi}{\sqrt{3}a}$ is the first Brillouin zone. As we have a curved surface, the local normals on the neighboring sites are no longer perfectly aligned and this misorientation also changes the transfer integral. The change can be calculated using the curvature tensor $b_{\alpha\beta}$ [19]. The result is

$$\frac{\delta t_a}{t} = -\frac{1}{2} b_{\gamma\beta} b_\alpha^\gamma \tau_a^\beta \tau_a^\alpha, \tag{19}$$

where the only nonzero term is $b_{xx} b_x^x = 1/R^2$. So we have

$$\frac{\delta t_1}{t} = 0, \tag{20}$$
$$\frac{\delta t_2}{t} = -\frac{1}{2} b_{xx} b_x^x (\tau_2^x)^2 = -\frac{1}{2R^2} (\tau_2^x)^2, \tag{21}$$
$$\frac{\delta t_3}{t} = -\frac{1}{2} b_{xx} b_x^x (\tau_3^x)^2 = -\frac{1}{2R^2} (\tau_3^x)^2. \tag{22}$$

With using the unit vectors we have $(\tau_2^x)^2 = (\tau_3^x)^2 = \frac{a^2}{4}$. We found the radius of the inner nanotube from the expression $2\pi R = Na$. The nonzero terms are $\frac{\delta t_2}{t} = \frac{\delta t_3}{t} = \frac{1}{2}(\frac{\pi}{N})^2$. The same holds for the outer nanotube. The parameters $\beta$, $\widetilde{\beta}$ can be expressed in the form

$$\widetilde{\beta} = 1 - \frac{\delta t_2}{t} = 1 - \frac{1}{2}\left(\frac{\pi}{9}\right)^2, \tag{23}$$

and

$$\beta = 1 - \frac{\delta t_2}{t} = 1 - \frac{1}{2}\left(\frac{\pi}{18}\right)^2. \tag{24}$$

Now we calculate the values $\epsilon$ and $\tilde{\epsilon}$ which are different because the inner and outer shell radii are different. Due to the curvature the coordinates of $\overrightarrow{\tau_i}$ in space are

$$\overrightarrow{\tau_1} = d(0; 1; 0),$$
$$\overrightarrow{\tau_2} = d\left(\frac{\sqrt{3}}{2}\cos\theta; -\frac{1}{2}; -\frac{\sqrt{3}}{2}\sin\theta\right),$$
$$\overrightarrow{\tau_3} = d\left(-\frac{\sqrt{3}}{2}\cos\theta; -\frac{1}{2}; -\frac{\sqrt{3}}{2}\sin\theta\right), \tag{25}$$

where $\sin\theta = a/4R$; $R$ is the radius of the nanotube. Now one can construct three hybrids along the three directions of the bonds. These directions are

$$\overrightarrow{e_1} = (0; 1; 0),$$
$$\overrightarrow{e_2} = \left(\frac{\sqrt{3}}{2}\cos\theta; -\frac{1}{2}; -\frac{\sqrt{3}}{2}\sin\theta\right),$$
$$\overrightarrow{e_3} = \left(-\frac{\sqrt{3}}{2}\cos\theta; -\frac{1}{2}; -\frac{\sqrt{3}}{2}\sin\theta\right). \tag{26}$$

The requirement of the orthonormality of the hybrid wave functions determines uniquely the fourth hybrid, denoted by $|\pi\rangle$, which corresponds to the $p_z$ orbital in graphite.

The hybridization of the $\sigma$ bonds therefore changes from the uncurved expression to

$$
\begin{aligned}
|\sigma_1\rangle &= s_1|s\rangle + \sqrt{1-s_1^2}|p_y\rangle,\\
|\sigma_2\rangle &= s_2|s\rangle + \sqrt{1-s_2^2}\\
&\quad\times\left(\frac{\sqrt{3}}{2}\cos\theta|p_x\rangle - \frac{1}{2}|p_y\rangle - \frac{\sqrt{3}}{2}\sin\theta|p_z\rangle\right),\\
|\sigma_3\rangle &= s_3|s\rangle + \sqrt{1-s_3^2}\\
&\quad\times\left(-\frac{\sqrt{3}}{2}\cos\theta|p_x\rangle - \frac{1}{2}|p_y\rangle - \frac{\sqrt{3}}{2}\sin\theta|p_z\rangle\right),\\
|\pi\rangle &= D_1|s\rangle + D_2|p_x\rangle + D_3|p_y\rangle + D_4|p_z\rangle. \qquad (27)
\end{aligned}
$$

The mixing parameters $s_i, D_j$ can be determined by the orthonormality conditions $\langle\sigma_i|\sigma_j\rangle = \delta_{ij}$, $\langle\pi|\sigma_i\rangle = 0$,$\langle\pi|\pi\rangle = 1$. We get

$$
\begin{aligned}
|\sigma_1\rangle &= \frac{1}{\sqrt{3\cos 2\theta}}|s\rangle + \sqrt{1-\frac{1}{3\cos 2\theta}}\ |p_y\rangle,\\
|\sigma_2\rangle &= \sqrt{\frac{3\cos 2\theta - 1}{3(\cos 2\theta + 1)}}|s\rangle + \sqrt{\frac{2}{3}}\frac{1}{\cos\theta}\\
&\quad\times\left(\frac{\sqrt{3}}{2}\cos\theta|p_x\rangle - \frac{1}{2}|p_y\rangle - \frac{\sqrt{3}}{2}\sin\theta|p_z\rangle\right),\\
|\sigma_3\rangle &= \sqrt{\frac{3\cos 2\theta - 1}{3(\cos 2\theta + 1)}}|s\rangle + \sqrt{\frac{2}{3}}\frac{1}{\cos\theta}\\
&\quad\times\left(-\frac{\sqrt{3}}{2}\cos\theta|p_x\rangle - \frac{1}{2}|p_y\rangle - \frac{\sqrt{3}}{2}\sin\theta|p_z\rangle\right),\\
|\pi\rangle &= \tan\theta\sqrt{\frac{3\cos 2\theta - 1}{3\cos 2\theta}}|s\rangle + \frac{\tan\theta}{\sqrt{3\cos 2\theta}}|p_y\rangle\\
&\quad + \frac{\sqrt{\cos 2\theta}}{\cos\theta}\ |p_z\rangle. \qquad (28)
\end{aligned}
$$

Now we can find the expression for the $\pi$ orbital to the lowest order in $a/R$

$$|\pi\rangle \approx \frac{a}{2\sqrt{6}R}|s\rangle + \frac{a}{4\sqrt{3}R}|p_y\rangle + |p_z\rangle, \qquad (29)$$

and so we get

$$\varepsilon = \langle\pi|H|\pi\rangle \approx \frac{a^2}{24R^2}\langle s|H|s\rangle + \frac{a^2}{48R^2}\langle p_y|H|p_y\rangle + \langle p_z|H|p_z\rangle. \qquad (30)$$

Due to $a/2R = \pi/N$, $(N = 9)$ we have

$$\tilde{\epsilon} = \frac{1}{6}\frac{\pi^2}{N^2}\langle s|H|s\rangle + \frac{1}{12}\frac{\pi^2}{N^2}\langle p_y|H|p_y\rangle + \langle p_z|H|p_z\rangle, \qquad (31)$$

and

$$\epsilon = \frac{1}{24}\frac{\pi^2}{N^2}\langle s|H|s\rangle + \frac{1}{48}\frac{\pi^2}{N^2}\langle p_y|H|p_y\rangle + \langle p_z|H|p_z\rangle. \qquad (32)$$

In the case $m = 3$ we find

$$E_{3,4}(k) = \epsilon \pm \gamma_0(1 - 2\beta\cos\frac{\sqrt{3}ka}{2} + \beta^2)^{\frac{1}{2}}, \qquad (33)$$

$$E_{11,12}(k) = \tilde{\epsilon} \pm \gamma_0(1 - 2\widetilde{\beta}\cos\frac{\sqrt{3}ka}{2} + \widetilde{\beta}^2)^{\frac{1}{2}}, \qquad (34)$$

where $k = 0$ is a Fermi point for both the inner and outer nanotubes in the case $\beta = \widetilde{\beta} = 1$. Nanotubes have no gap and have a semiconductor character. If we impose a curvature correction, we get a gap

$$E_g = 2(1-\beta) = \gamma_0\left(\frac{\pi}{2N}\right)^2 = \frac{\gamma_0}{4}\left(\frac{a}{2R}\right)^2, \qquad (35)$$

for the outer nanotube and

$$E_g = 2(1-\widetilde{\beta}) = \gamma_0\left(\frac{\pi}{N}\right)^2 = \frac{\gamma_0}{4}\left(\frac{a}{R}\right)^2, \qquad (36)$$

for the inner nanotube. Here $R$ is the radius of the inner tube and $2R$ is the radius of the outer tube. So we get the same gap as was computed in [20] where the rehybridized orbital method was used. For $\gamma_0 \approx 3$ eV we get $E_g \approx 0.365$ eV for the inner tube and $E_g \approx 0.091$ eV for the outer tube. Now we want to estimate the difference between "Fermi levels" of the inner and the outer shell. We have [21]

$$\langle s|H|s\rangle \approx -12 \text{ eV}, \qquad (37)$$

$$\langle p_y|H|p_y\rangle \approx -4 \text{ eV}, \qquad (38)$$

and the difference is

$$
\begin{aligned}
\epsilon - \tilde{\epsilon} &= \frac{1}{6}\left(\left(\frac{\pi}{2N}\right)^2 - \left(\frac{\pi}{N}\right)^2\right)\langle s|H|s\rangle\\
&\quad + \frac{1}{12}\left(\left(\frac{\pi}{2N}\right)^2 - \left(\frac{\pi}{N}\right)^2\right)\langle p_y|H|p_y\rangle. \qquad (39)
\end{aligned}
$$

From the expression above we finally get the value for the energy gap

$$\epsilon - \tilde{\epsilon} \approx 0.21 \text{ eV}. \qquad (40)$$

Now we use the eigenstates $\psi_i$ to find the solution when the interaction between shells is imposed. We assume the symmetric geometry of zig-zag DWNT. It means that the atoms $A, A_1$ and $B, B_1$ are directly one above another in the neighboring shells [10]. We take into account only the interactions

$$W_{A,A_1} = W_{B,B_1} = \frac{\gamma_0}{8}. \qquad (41)$$

We look for solution in the form

$$\Psi = \sum_{i=1}^{12}\zeta_i\psi_i. \qquad (42)$$

We have secular equations

$$\sum_{j=1}^{12}\langle\psi_i|H|\psi_j\rangle\zeta_j = \tilde{E}\zeta_i, \qquad (43)$$

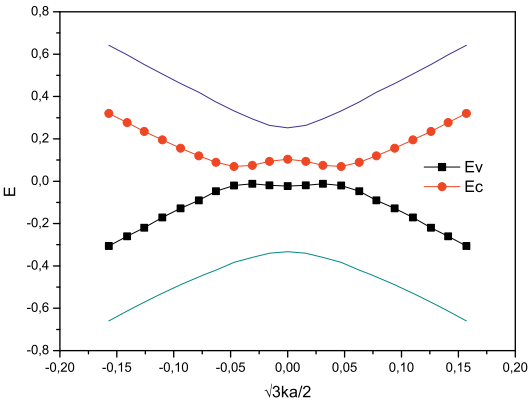


**Fig. 3.** (Color online) Spectra of zigzag DWNT with the intertube interactions.

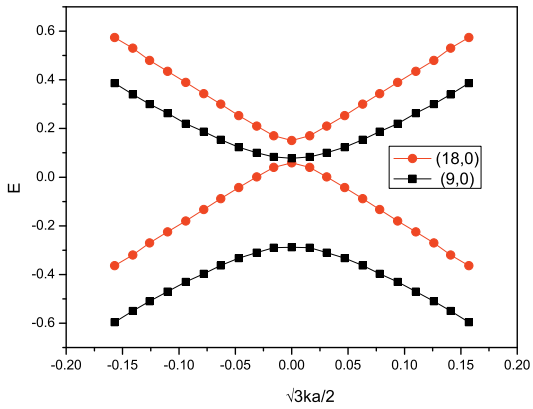


**Fig. 4.** (Color online) Spectra of zigzag DWNT in the absence of the intertube interactions.

where

$$\langle\psi_i|H|\psi_j\rangle = \delta_{ij}E_i, \tag{44}$$

for $i,j = 1,...8$ and $i,j = 9,...12$, and the interaction between shells is described by the terms $\langle\psi_i|H|\psi_j\rangle$ for $i = 1,...8$ ; $j = 9,...12$ and vice versa. We have, for instance,

$$\langle\psi_9|H|\psi_1\rangle = \frac{1}{4\sqrt{2}}\frac{\gamma_0}{8}\left(1+e^{i(\varphi_5-\varphi_1)}\right), \tag{45}$$

$$\langle\psi_9|H|\psi_2\rangle = \frac{1}{4\sqrt{2}}\frac{\gamma_0}{8}\left(1-e^{i(\varphi_5-\varphi_1)}\right). \tag{46}$$

We get the eigenvalues $\tilde{E}_i$ with eigenvectors which can be expressed in the form

$$\Psi_i = \sum_{j=1}^{12}\zeta_{i,j}\psi_j. \tag{47}$$

The eigenvalues of equation (55) for some values of $\sqrt{3}ka/2$ near the point $k = 0$ are depicted in Figure 3 where $E_c$ and $E_v$ are conductive and valence band. The band structure for zig-zag DWNT without intertube interactions is also shown for comparison (Fig. 4). At the point $k = 0$ we get the wave function of the valence band

$$\Psi_v \simeq -0.6\psi_3 + 0.8\psi_{11}, \tag{48}$$

$\psi_3(\psi_{11})$ is $\pi^*$ state of the outer(inner) nanotube. We get a minimum gap $E_g \simeq 90$ meV between the valence and conductive band of the DWNTs at the wave vectors $\sqrt{3}ka/2 \simeq \pm 0.05$. At these points the wave function has the form

$$\Psi_v \simeq -0.263i\psi_3 + 0.838\psi_4 - (0.14+0.45i)\psi_{11} + (0.29-0.09i)\psi_{12}, \tag{49}$$

$\psi_4(\psi_{12})$ is $\pi$ state of the outer(inner) nanotube. We calculated also the electronic structure of $(8,0)$–$(16,0)$ and $(10,0)$–$(20,0)$ DWNTs. The energy gaps are collected in the Tables 1 and 2. To compute the gaps $\Delta$ we used formula (19). The gaps denoted by $\Delta_{KM}$ are computed with formula used in [22]; $\Delta_{TB}$ are gaps calculated in the simple zone folding tight-binding approximation where the curvature effects are not taken into account. We compare our results with the previous computed energy gaps. For $(8,0)$–$(16,0)$ DWNTs we get a gap which is significantly greater than that computed by density functional theory (DFT). It is mainly caused by that the tight-bounding method gives greater gaps for nanotubes with a very small diameter than the DFT computations. Another reason is that we describe DWNTs as one unified system where single nanotubes partially lose their individual characteristics due to the interactions. For $(10,0)$–$(20,0)$ DWNTs we get a similar gap as in [25].

**Table 1.** The values of the minimum energy gaps for different types of zig-zag SWNTs. The values are calculated in eV. $\Delta$ and $\Delta_{KM}$ are the gaps computed in the present paper. The values for comparison $\Delta_{TB}$, $\Delta_{DFT}$ are computations from simple zone tight-binding and density functional theory [28].

| $SWNT$ | $\Delta$ | $\Delta_{KM}$ | $\Delta_{TB}$ | $\Delta_{DFT}$ |
|---|---|---|---|---|
| $(8,0)$ | 1.752 | 1.496 | 1.42 | 0.59 |
| $(9,0)$ | 0.37 | 0.093 | 0 | 0.096 |
| $(10,0)$ | 0.705 | 0.966 | 1.07 | 0.77 |
| $(16,0)$ | 0.538 | 0.634 | 0.67 | 0.54 |
| $(18,0)$ | 0.091 | 0.023 | 0 | 0.013 |
| $(20,0)$ | 0.619 | 0.568 | 0.56 | 0.50 |

**Table 2.** The values of the minimum energy gaps for different types of zig-zag DWNTs. The values are calculated in eV, $\Delta_{DFT}$ is taken from [27]

| $DWNT$ | $\Delta$ | $\Delta_{KM}$ | $\Delta_{DFT}$ |
|---|---|---|---|
| $(8,0)$–$(16,0)$ | 1.234 | 1.080 | 0.35 |
| $(9,0)$–$(18,0)$ | 0.09 | 0.061 | – |
| $(10,0)$–$(20,0)$ | 0.494 | 0.676 | – |

## 3 (5, 5)–(10, 10) armchair tubules

We can make similar calculations of electronic spectra also in the case of armchair double-layer nanotubes. The system is characterized by the same Hamiltonian as in the previous section. We can define the vectors connecting the

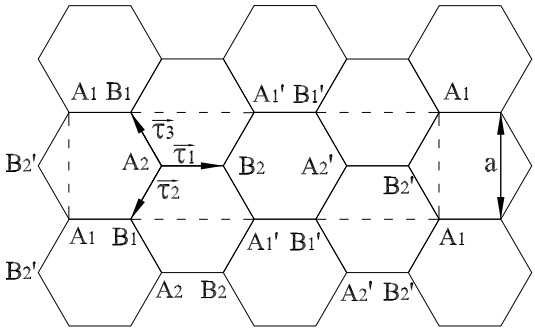


**Fig. 5.** The outer shell part of the unit cell in the case of armchair nanotubes.

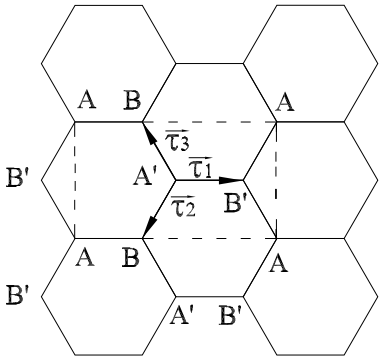


**Fig. 6.** The inner shell part of the unit cell in the case of armchair nanotubes.

nearest neighbor carbon atoms for armchair nanotubes in the form:

$$\begin{aligned}\overrightarrow{\tau_1} &= a(\frac{1}{\sqrt{3}};0),\\ \overrightarrow{\tau_2} &= a(-\frac{1}{2\sqrt{3}};-\frac{1}{2}),\\ \overrightarrow{\tau_3} &= a(-\frac{1}{2\sqrt{3}};\frac{1}{2}).\end{aligned} \tag{50}$$

The distance between atoms in the unit cell is also $|\overrightarrow{\tau_i}| = \frac{a}{\sqrt{3}}$.

Now we define the intratube hopping integrals

$$\begin{aligned}\langle\varphi^{out}(r-A_1)|H|\varphi^{out}(r-B_1)\rangle &= \gamma_0\alpha,\\ \langle\varphi^{out}(r-A_1)|H|\varphi^{out}(r-B_2')\rangle &= \gamma_0\beta,\end{aligned} \tag{51}$$

and

$$\begin{aligned}\langle\varphi^{in}(r-A)|H|\varphi^{in}(r-B)\rangle &= \gamma_0\widetilde{\alpha},\\ \langle\varphi^{in}(r-A)|H|\varphi^{in}(r-B')\rangle &= \gamma_0\widetilde{\beta},\end{aligned} \tag{52}$$

where $\gamma_0$ is the hoping integral in the graphene and $\alpha(\widetilde{\alpha})$, $\beta(\widetilde{\beta})$ are parameters which describe the dependence of hopping integrals on the surface curvature. From Figures 5 and 6 we get the system of equations as describing in Appendix B.

At the beginning we neglect the intertube interactions in the equations described in Appendix B. We get a set of equations which can be decoupled. One set for the outer shell and the other for the inner shell. The electronic spectra and eigenstate for the outer shell can be expressed in the form

$$E_{1,2}(k)=\epsilon\pm\gamma_0\left(\alpha^2+4\alpha\beta\cos\frac{m\pi}{5}\cos\frac{ka}{2}+4\beta^2\cos^2\frac{ka}{2}\right)^{\frac{1}{2}},$$

$$\psi_{1,2}=\frac{1}{\sqrt{8}}\left(1;\pm e^{-i\varphi_1};1;\pm e^{-i\varphi_1},1;\pm e^{-i\varphi_1};1;\pm e^{-i\varphi_1}\right) \tag{53}$$

$$E_{3,4}(k)=\epsilon\pm\gamma_0\left(\alpha^2-4\alpha\beta\cos\frac{m\pi}{5}\cos\frac{ka}{2}+4\beta^2\cos^2\frac{ka}{2}\right)^{\frac{1}{2}},$$

$$\psi_{3,4}=\frac{1}{\sqrt{8}}\left(1;\pm e^{-i\varphi_2};-1;\mp e^{-i\varphi_2},1;\pm e^{-i\varphi_2};-1;\mp e^{-i\varphi_2}\right) \tag{54}$$

$$E_{5,6}(k)=\epsilon\pm\gamma_0\left(\alpha^2+4\alpha\beta\sin\frac{m\pi}{5}\cos\frac{ka}{2}+4\beta^2\cos^2\frac{ka}{2}\right)^{\frac{1}{2}},$$

$$\psi_{5,6}=\frac{1}{\sqrt{8}}\left(1;\pm e^{-i\varphi_3};-i;\mp ie^{-i\varphi_3},-1;\mp e^{-i\varphi_3};i;\pm ie^{-i\varphi_3}\right) \tag{55}$$

$$E_{7,8}(k)=\epsilon\pm\gamma_0\left(\alpha^2-4\alpha\beta\sin\frac{m\pi}{5}\cos\frac{ka}{2}+4\beta^2\cos^2\frac{ka}{2}\right)^{\frac{1}{2}},$$

$$\psi_{7,8}=\frac{1}{\sqrt{8}}\left(1;\pm e^{-i\varphi_4};i;\pm ie^{-i\varphi_4},-1;\mp e^{-i\varphi_4};-i;\mp ie^{-i\varphi_4}\right). \tag{56}$$

The electronic spectra for the inner nanotubes was found in the form

$$E_{9,10}(k)=\tilde{\epsilon}\pm\gamma_0\left(\widetilde{\alpha}^2+4\widetilde{\alpha}\widetilde{\beta}\cos\frac{m\pi}{5}\cos\frac{ka}{2}+4\widetilde{\beta}^2\cos^2\frac{ka}{2}\right)^{\frac{1}{2}},$$

$$\psi_{9,10}=\frac{1}{\sqrt{4}}\left(1;\pm e^{-i\varphi_5};1;\pm e^{-i\varphi_5}\right) \tag{57}$$

$$E_{11,12}(k)=\tilde{\epsilon}\pm\gamma_0\left(\widetilde{\alpha}^2-4\widetilde{\alpha}\widetilde{\beta}\cos\frac{m\pi}{5}\cos\frac{ka}{2}+4\widetilde{\beta}^2\cos^2\frac{ka}{2}\right)^{\frac{1}{2}},$$

$$\psi_{11,12}=\frac{1}{\sqrt{4}}\left(1;\pm e^{-i\varphi_6};-1;\mp e^{-i\varphi_6}\right). \tag{58}$$

From the boundary condition $k_xL = 2\pi m$, $L = N3d$ where $d = a/\sqrt{3}$ is the nearest neighbor bond length we get $k_x = \frac{2\pi m}{3dN} = \frac{2\pi m}{\sqrt{3}Na}$, $m = 0, 1, ...N-1$; $3d$ is the length of the unit cell in the $x$-direction. Here $k_y = k$ and $-\frac{\pi}{a} < k < \frac{\pi}{a}$ is the first Brillouin zone. In this case, we assume that $N = 5$ for the above spectrum.

The value for the parameter $\widetilde{\alpha}$ and $\widetilde{\beta}$ can be found from the expressions $\widetilde{\alpha} = 1 - \frac{1}{2}b_{xx}b_x^x(\tau_1^x)^2 = 1 - \frac{1}{2R^2}\frac{a^2}{3}$ and $\widetilde{\beta} = 1 - \frac{1}{2}b_{xx}b_x^x(\tau_2^x)^2 = 1 - \frac{1}{2R^2}\frac{a^2}{12}$. The radius for the inner, outer nanotube can be found from the expressions $2\pi R = N3d = \sqrt{3}Na$, $2\pi R = N6d$, respectively. Now we make a correction of transfer integral caused by the curvature of nanotubes

$$\widetilde{\beta} = 1 - \frac{1}{2}(\frac{\pi}{3N})^2; \quad \beta = 1 - \frac{1}{8}(\frac{\pi}{3N})^2, \tag{59}$$

$$\widetilde{\alpha} = 1 - 2(\frac{\pi}{3N})^2; \quad \alpha = 1 - \frac{1}{2}(\frac{\pi}{3N})^2. \tag{60}$$

We calculate the values $\epsilon$ and $\tilde{\epsilon}$. Due to the curvature the coordinates of $\overrightarrow{\tau_i}$ in space are

$$\begin{aligned}
\overrightarrow{\tau_1} &= d(\cos\theta; 0; -\sin\theta),\\
\overrightarrow{\tau_2} &= d\left(-\frac{1}{2}\cos\vartheta; -\frac{\sqrt{3}}{2}; -\frac{1}{2}\sin\vartheta\right),\\
\overrightarrow{\tau_3} &= d\left(-\frac{1}{2}\cos\vartheta; \frac{\sqrt{3}}{2}; -\frac{1}{2}\sin\vartheta\right),
\end{aligned} \tag{61}$$

where $\sin\theta = d/2R$ and $\sin\vartheta = d/4R$; $R$ is the radius of the nanotube. In a similar way, as in the previous section, we get

$$\begin{aligned}
|\sigma_1\rangle &= \frac{\cos(\theta+\vartheta)}{\sqrt{2+\cos^2(\theta+\vartheta)}}\,|s\rangle\\
&\quad + \sqrt{\frac{2}{2+\cos^2(\theta+\vartheta)}}\,\left(\cos\theta|p_x\rangle - \sin\theta|p_z\rangle\right),\\
|\sigma_2\rangle &= \frac{1}{\sqrt{3}}|s\rangle + \sqrt{\frac{2}{3}}\left(-\frac{1}{2}\cos\vartheta|p_x\rangle - \frac{\sqrt{3}}{2}|p_y\rangle - \frac{1}{2}\sin\vartheta|p_z\rangle\right),\\
|\sigma_3\rangle &= \frac{1}{\sqrt{3}}|s\rangle + \sqrt{\frac{2}{3}}\left(-\frac{1}{2}\cos\vartheta|p_x\rangle + \frac{\sqrt{3}}{2}|p_y\rangle - \frac{1}{2}\sin\vartheta|p_z\rangle\right),\\
|\pi\rangle &= \sqrt{\frac{2}{3}}\frac{\sin(\theta+\vartheta)}{\sqrt{2+\cos^2(\theta+\vartheta)}}|s\rangle\\
&\quad + \frac{2\sin\theta - \sin\vartheta\cos(\theta+\vartheta)}{\sqrt{6+3\cos^2(\theta+\vartheta)}}|p_x\rangle\\
&\quad + \frac{2\cos\theta + \cos\vartheta\cos(\theta+\vartheta)}{\sqrt{6+3\cos^2(\theta+\vartheta)}}|p_z\rangle.
\end{aligned} \tag{62}$$

Now we can find the expression for the $\pi$ orbital to the lowest order in $d/R$

$$|\pi\rangle \approx \frac{\sqrt{2}d}{4R}|s\rangle + \frac{d}{4R}\,|p_x\rangle + |p_z\rangle. \tag{63}$$

Due to $3dN = 2\pi R$ we get

$$|\pi\rangle \approx \frac{\sqrt{2}\pi}{6N}|s\rangle + \frac{\pi}{6N}\,|p_x\rangle + |p_z\rangle, \tag{64}$$

and so

$$\begin{aligned}
\varepsilon = \langle\pi|H|\pi\rangle \approx\ & \frac{1}{18}\left(\frac{\pi}{N}\right)^2\langle s|H|s\rangle\\
&+ \frac{1}{36}\left(\frac{\pi}{N}\right)^2\langle p_x|H|p_x\rangle + \langle p_z|H|p_z\rangle.
\end{aligned} \tag{65}$$

From this expression we derive, if $(N = 5)$,

$$\tilde{\epsilon} = \frac{1}{18}\left(\frac{\pi}{N}\right)^2\langle s|H|s\rangle + \frac{1}{36}\left(\frac{\pi}{N}\right)^2\langle p_x|H|p_x\rangle + \langle p_z|H|p_z\rangle, \tag{66}$$

and

$$\epsilon = \frac{1}{18}\left(\frac{\pi}{2N}\right)^2\langle s|H|s\rangle + \frac{1}{36}\left(\frac{\pi}{2N}\right)^2\langle p_x|H|p_x\rangle + \langle p_z|H|p_z\rangle. \tag{67}$$

The energy levels $E_{3,4}$ and $E_{11,12}$ define the Fermi point for $m = 0$. We have

$$E_{3,4}(k) = \epsilon \pm \gamma_0|\alpha - 2\beta\cos\frac{ka}{2}|, \tag{68}$$

$$E_{11,12}(k) = \tilde{\epsilon} \pm \gamma_0|\widetilde{\alpha} - 2\widetilde{\beta}\cos\frac{ka}{2}|, \tag{69}$$

and the Fermi point is defined by the equations

$$\widetilde{\alpha} - 2\widetilde{\beta}\cos\frac{ka}{2} = 0, \tag{70}$$

for the inner shell, and

$$\alpha - 2\beta\cos\frac{ka}{2} = 0, \tag{71}$$

for the outer shell, respectively. By virtue of $\beta \geq \alpha(\tilde{\beta} \geq \tilde{\alpha})$ the curvature does not open a gap in the case of single nanotubes. Using the values $\langle s|H|s\rangle \approx -12$ eV and $\langle p_x|H|p_x\rangle \approx -4$ eV in the following expression:

$$\begin{aligned}
\epsilon - \tilde{\epsilon} =\ & \frac{1}{18}\left(\left(\frac{\pi}{2N}\right)^2 - \left(\frac{\pi}{N}\right)^2\right)\langle s|H|s\rangle\\
&+ \frac{1}{36}\left(\left(\frac{\pi}{2N}\right)^2 - \left(\frac{\pi}{N}\right)^2\right)\langle p_x|H|p_x\rangle,
\end{aligned} \tag{72}$$

we find

$$\epsilon - \tilde{\epsilon} \approx 0.23 \text{ eV}. \tag{73}$$

Now we use the eigenstates $\psi_i$ to find the solution when the interaction between shells is imposed. Similarly, as in the previous case, we look for the solution in the form

$$\Psi = \sum_{i=1}^{12}\zeta_i\psi_i. \tag{74}$$

We have secular equations

$$\sum_{j=1}^{12}\langle\psi_i|H|\psi_j\rangle\zeta_j = \tilde{E}\zeta_i. \tag{75}$$

We take into account all intertube interactions between atoms which have a distance $d_{ij}$ less than 4.2 Å similarly

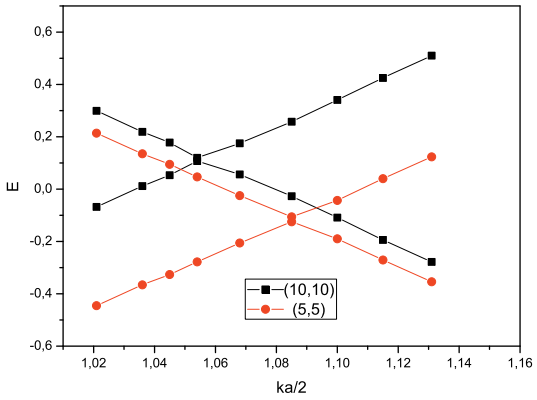


**Fig. 7.** (Color online) Spectra of armchair DWNT in the absence of the intertube interactions.

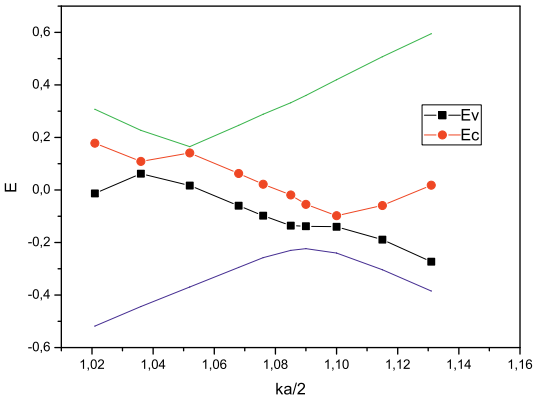


**Fig. 8.** (Color online) Spectra of armchair DWNT with the intertube interactions in symmetric case.

as in [15,16]. We use the value $\xi = 3.466$ for the intertube distance in the numerical computations. We compute spectra for three different geometries. The first case was symmetric geometry where the atoms $B_2'(A_2)$ occupy a position directly above $A'(B')$, respectively. In the second case, we shift the inner shell axially by 0.612 Å and in the third case, we rotate the inner shell by 6° from the symmetric orientation. We get the eigenvalues $\tilde{E}_i$ with eigenvectors which can be expressed in the form

$$\Psi_i = \sum_{j=1}^{12} \zeta_{i,j}\psi_j. \qquad (76)$$

The spectra for some values of $ka/2$ near the Fermi points of single nanotubes are depicted in Figure 7. The point $ka/2 = 1.086$ is the Fermi point of the isolated inner nanotube. The point $ka/2 = 1.057$ is the Fermi point of the isolated outer nanotube. Approximately, from point $ka/2 = 1.054$ to point 1.095 the $\tilde{E}_{11}$ levels are below the $\tilde{E}_4$ level. So in the armchair DWNT the state $\Psi_{11}$ is occupied at these points. The state $\Psi_{11}$ is some mixture of the states $\psi_i$. For example, for the point $ka/2 = 1.083$ we have that the main part of $\Psi_{11}$ is $\psi_{11}$ which is $\pi^*$ state of the inner tube.

We get that electrons which are localized in the outer nanotubes in the case without interaction between shells

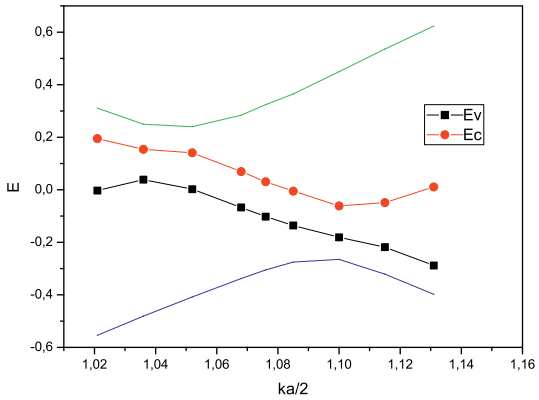


**Fig. 9.** (Color online) Spectra of armchair DWNT with the intertube interactions with shift of y-axes of inner tube about $\sqrt{3}b/4$ Å.

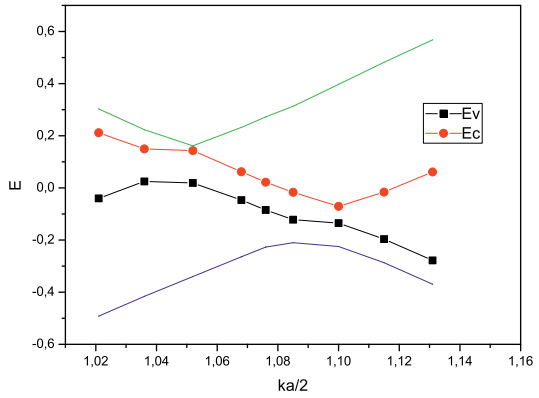


**Fig. 10.** (Color online) Spectra of armchair DWNT with the intertube interactions with rotation of inner tube about 6 angle.

(or in the case of single nanotubes) are now localized in the inner nanotubes in the state which is unoccupied in the single nanotubes. Figures 8–10 describe how the shift and rotation of the inner nanotube, similarly as in [15], influence the energy gap between conductance and valence bands in the DWNTs armchair nanotube where $E_c$ and $E_v$ are conductive and valence bands. We get similar results for $(4,4)$–$(8,8)$ and $(6,6)$–$(12,12)$ DWNTs.

## 4 Conclusion

In the present work, we take into account that the Fermi levels of the individual nanotubes which create the double wall nanotubes are different. This difference is very important in the double wall nanotubes with small diameters. The interplay between energy difference of the Fermi levels of the individual nanotubes and the energy gap between valence and conducting band of individual nanotubes have a strong effect on the conductivity of double wall nanotubes [23–25]. The important parameter is also a difference of wave vectors $k_F$ of the individual nanotubes.

To compute the influence of a curvature of the surface on the matrix elements of the secular equation, we used two methods. The rehybridization of the $\pi$ orbital method was used for the computation of diagonal matrix elements which define the Fermi levels of single nanotubes. To compute the nondiagonal matrix element, we used the curvature tensor $b_{ij}$. In the present work, we get the same gap as in [20] which was computed by the rehybridized method for single wall zig-zag nanotubes. The gap is by a factor of 4 larger than that computed in the previous study [22]. The reason is that we get analytically a 4 time bigger term $\delta t_i/t$. The curvature of the surface opens the gap in the zig-zag SWNTs but does not open the gap in the armchair SWNTs. The Fermi level of the outer shell is about 0.21 eV higher than the Fermi level of the inner shell in the case of $(9,0)$–$(18,0)$ zig-zag DWNTs. In the case of zig-zag DWNTs, the curvature does not shift the minimum of the conductance band and maximum of the valence band of the individual nanotubes. The result is that these DWNTs are the semiconductor. The electronic structure of the $(9,0)$–$(18,0)$ DWNTs in the absence of the intertube interactions is shown in Figure 4. Due to the difference in Fermi levels of individual nanotubes the valence states are not symmetric to conduction states about the Fermi level. We have a gap $E_g = 25$ meV between the valence band of the outer shell and the conductive band of the inner shell. The difference in the Fermi levels of individual nanotubes has not been taken into account in [10]. They have symmetric valence states to the conduction states, and the energy gap $E_g$ is associated with outer $(18,0)$ nanotubes in the absence of the intertube interaction. We get a minimum gap between the valence and conductive band at the points $\sqrt{3}ka/2 \simeq \pm 0.05$ and this energy gap has value $E_g = 90$ meV when the intertube interactions are imposed. We also compute the energy gaps of $(8,0)$–$(16,0)$ and $(10,0)$–$(20,0)$ zig-zag DWNTs. For $(8,0)$–$(16,0)$ DWNTs we get a significantly greater gap than is predicted by DFT calculations. It is mainly due to difference in the energy gaps of $(8,0)$ SWNTs. DFT calculations predict energy gaps 0.6 eV. Quasiparticle corrections open the gap to 1.75 eV [26]. A similar gap is predicted in the present paper. The values of the minimum energy gaps for different types of zig-zag SWNTs and DWNTs are collected in Tables 1 and 2.

The Fermi level of the outer shell is about 0.23 eV higher than the Fermi level of the inner shell for $(5,5)$–$(10,10)$ armchair DWNTs. The result is that in the armchair DWNTs part of electrons from the valence band of the outer shell comes to the conductance band of the inner shell. The inner shell will have a negative charge and will have electron conductivity, and the outer shell will have a positive charge and will have hole conductivity. In the case of armchair SWNTs, the Fermi points are shifted and the shift depends on the curvature. Since the $\frac{\alpha}{2\beta}$ is bigger than $\frac{\tilde{\alpha}}{2\tilde{\beta}}$, the Fermi point $k_F$ of the outer nanotube is smaller than the wave vector $k_F$ of the Fermi point of the inner nanotube. The highest occupied state is located above the lowest unoccupied state in the case of the armchair DWNT. The differences are 0.16 eV in the symmetric geometry, 0.1 eV when inner nanotube is shifted in the direction of the axes and 96 meV in the case of the rotational displacement of the inner with respect to the outer tube. So armchair DWNTs have a semimetallic character. We get the same character of the conductivity in all computed geometries for the armchair $(5,5)$–$(10,10)$ nanotube. It means that the conductivity does not strongly depend on the relative position of individual shells. We get similar results, as in [3,4], for the asymmetric geometry of $(5,5)$–$(10,10)$ armchair nanotube, but we have the inverse asymmetry of the electronic spectra. In our model we get the asymmetry because the Fermi level of the outer nanotube is higher than the Fermi level of the inner nanotube, and the wave vector $k_F$ of the Fermi level of the outer nanotube is smaller than the wave vector of the Fermi level of the inner nanotube (Fig. 8). We get similar results also for $(4,4)$–$(8,8)$ and $(6,6)$–$(12,12)$ DWNTs where the highest occupied state is 0.217 eV above the lowest unoccupied state in the case of $(4,4)$–$(8,8)$ DWNTs and 0.12 eV in the case of $(6,6)$–$(12,12)$ DWNTs.

The main reason why there is a difference in the character of the conductivity of armchair and zig-zag double wall nanotubes is the absence of the shift of the wave vector $k$ where the individual zig-zag nanotubes have a minimal gap. So zig-zag DWNTs are semiconductors. We have a maximum of the valence band of the outer armchair nanotube higher than a minimum of the conductive band of the inner nanotube in the armchair DWNTs. There is no energy gap in armchair nanotubes but there is a shift of $k_F$. Those are the main reasons why the armchair double wall nanotubes with a small radius are semimetal. We can also conclude that the shift and rotation of the inner nanotube do not influent largely the main characteristics of the DWNTs armchair nanotubes; therefore, they are stable with their semimetallic character. It would be interesting to test this prediction in experiment.

Generally, we can say that the conductivity depends on the relative position of the wave vectors $k$ where the individual nanotubes have a minimum gap. If there is no shift, the DWNTs are semiconductors. Zig-zag SWNTs have a minimum gap at point $\Gamma$. It means that from our prediction all zig-zag DWNTs ought to be semiconductors. It is partially supported in [25]. On the other hand, if there is a shift in the wave vectors where the individual nanotubes have a minimal gap depending on the mutual positions of the Fermi levels and the energy gap width of individual nanotubes, the DWNT can be semimetal or semiconductor. The examples are $(5,5)$–$(10,10)$ DWNTs where the shift is caused by curvature and $(4,2)$–$(10,5)$ DWNTs where individual nanotubes have gap minima at the points $X$ and $\Gamma$ [27]. We have shown that the difference in the Fermi level energies and mixing of orbitals localized on the outer and inner nanotubes cause the charge transfer from outer to inner tubules. We do not take into account that charge transfer between the outer and inner tubules create an electric field between these tubules. So not all electrons can transfer from the outer shell to the inner shell, as is predicted by the present study. Assumption of this effect can make a reconstruction of the

electronic spectra of DWNTs. This is important mainly in the DWNTs where the inner nanotube has a very small diameter. The result can be metallic character of zig-zag DWNTs with $(7,0)$ and $(5,0)$ inner nanotube, as is predicted in [6,7,27]. Our calculations predict semiconducting character of $(9,0)$–$(18,0)$ DWNTs similarly to [3,10] and contrary to [6]. It ought to be resolved.

If inner shell has a radius about 7 Å and more, the difference between Fermi energy of the outer and the inner tubules is small. So the charge transfer is not significant. The lower the minimum of the $\pi^*$ state of the inner nanotube in comparison with the maximum of the $\pi$ state of the outer nanotube the bigger charge transfer is. If individual nanotubes have metallic character, the charge transfer will be greater then in the case of DWNTs where one or both of the nanotubes are semiconductor. It means for instance that the charge transfer is smaller in the case of zig-zag DWNTs than in the case of armchair DWNTs with similar radius. Charge transfer is from the outer to the inner nanotube because Fermi level of the outer nanotube is higher then Fermi level of the inner nanotube.

From equation (71) we get the following formula for the Fermi wave vector $k_F$ of the armchair SWNT;

$$k_F = \frac{2}{a} \arccos \frac{1 - \frac{1}{2}\left(\frac{d}{R}\right)^2}{2\left(1 - \frac{1}{8}\left(\frac{d}{R}\right)^2\right)}. \quad (77)$$

For a large radius the Fermi wave vector is located at $k_F(R \to \infty) = 2\pi/3a$. As a diameter decreases, the position of $k_F$ shifts from $k_F(R \to \infty)$ towards the bigger wave vectors. The DFT calculations predict the opposite shift [28]. Parameter $\alpha$ is smaller than parameter $\beta$. It means that because of curvature the hopping integral in the $\boldsymbol{\tau}_1$ direction is smaller than the hopping integrals in the $\boldsymbol{\tau}_2$ and $\boldsymbol{\tau}_3$ directions. This is the reason why we get the shift of $k_F$ towards the bigger wave vector with decreasing of the radius of the nanotube. We expect that less symmetric DWNTs have no such stable characteristic when we change a relative position of the outer and inner nanotubes. The oscillation character of a energy gap will not exist in the case of less symmetric DWNTs. The understanding how the rotation of the inner nanotube in different types of DWNTs influences electronic properties of this type of nanostructures is needed to design a new type of nanomotors [29].

The authors thank Prof. V.A. Osipov for helpful discussions and advice. The work was supported by VEGA grant 2/7056/27 of the Slovak Academy of Sciences and by the Science and Technology Assistance Agency under contract No. APVV 0509-07.

## Appendix A

In a tight-binding approximation for the case of zig-zag tubules we get the following systems of equations: for the outer shell

$$\epsilon C_{A_1} + H_{A_1B_2}C_{B_2} + H_{A_1B_2'}C_{B_2'} + H_{A_1B_1}C_{B_1} + \sum_\lambda W_{A_1,\lambda}C_\lambda = EC_{A_1}, \quad (78)$$

where $H_{A_1B_2} = \gamma_0\beta e^{i\vec{k}\vec{\tau}_2}$; $H_{A_1B_2'} = \gamma_0\beta e^{i\vec{k}\vec{\tau}_3}$; $H_{A_1B_1} = \gamma_0 e^{i\vec{k}\vec{\tau}_1}$.

$$\epsilon C_{B_1} + H_{B_1A_1}C_{A_1} + H_{B_1A_2'}C_{A_2'} + H_{B_1A_2}C_{A_2} + \sum_\lambda W_{B_1,\lambda}C_\lambda = EC_{B_1}, \quad (79)$$

where $H_{B_1A_1} = \gamma_0 e^{-i\vec{k}\vec{\tau}_1}$; $H_{B_1A_2'} = \gamma_0\beta e^{-i\vec{k}\vec{\tau}_2}$; $H_{B_1A_2} = \gamma_0\beta e^{-i\vec{k}\vec{\tau}_3}$.

$$\epsilon C_{A_2} + H_{A_2B_1}C_{B_1} + H_{A_2B_2}C_{B_2} + H_{A_2B_1'}C_{B_1'} + \sum_\lambda W_{A_2,\lambda}C_\lambda = EC_{A_2}, \quad (80)$$

where $H_{A_2B_2} = \gamma_0 e^{i\vec{k}\vec{\tau}_1}$; $H_{A_2B_1} = \gamma_0\beta e^{i\vec{k}\vec{\tau}_3}$; $H_{A_2B_1'} = \gamma_0\beta e^{i\vec{k}\vec{\tau}_2}$.

$$\epsilon C_{B_2} + H_{B_2A_1}C_{A_1} + H_{B_2A_1'}C_{A_1'} + H_{B_2A_2}C_{A_2} + \sum_\lambda W_{B_2,\lambda}C_\lambda = EC_{B_2}, \quad (81)$$

where $H_{B_2A_1} = \gamma_0\beta e^{-i\vec{k}\vec{\tau}_2}$; $H_{B_2A_1'} = \gamma_0\beta e^{-i\vec{k}\vec{\tau}_3}$; $H_{B_2A_2} = \gamma_0 e^{-i\vec{k}\vec{\tau}_1}$.

$$\epsilon C_{B_1'} + H_{B_1'A_2}C_{A_2} + H_{B_1'A_2'}C_{A_2'} + H_{B_1'A_1'}C_{A_1'} + \sum_\lambda W_{B_1',\lambda}C_\lambda = EC_{B_1'}, \quad (82)$$

where $H_{B_1'A_2} = \gamma_0\beta e^{-i\vec{k}\vec{\tau}_2}$; $H_{B_1'A_2'} = \gamma_0\beta e^{-i\vec{k}\vec{\tau}_3}$; $H_{B_1'A_1'} = \gamma_0 e^{-i\vec{k}\vec{\tau}_1}$.

$$\epsilon C_{A_2'} + H_{A_2'B_1'}C_{B_1'} + H_{A_2'B_2'}C_{B_2'} + H_{A_2'B_1}C_{B_1} + \sum_\lambda W_{A_2',\lambda}C_\lambda = EC_{A_2'}, \quad (83)$$

where $H_{A_2'B_1'} = \gamma_0\beta e^{i\vec{k}\vec{\tau}_3}$; $H_{A_2'B_2'} = \gamma_0 e^{i\vec{k}\vec{\tau}_1}$; $H_{A_2'B_1} = \gamma_0\beta e^{i\vec{k}\vec{\tau}_2}$.

$$\epsilon C_{B_2'} + H_{B_2'A_2'}C_{A_2'} + H_{B_2'A_1'}C_{A_1'} + H_{B_2'A_1}C_{A_1} + \sum_\lambda W_{B_2',\lambda}C_\lambda = EC_{B_2'}, \quad (84)$$

where $H_{B_2'A_2'} = \gamma_0 e^{-i\vec{k}\vec{\tau}_1}$; $H_{B_2'A_1'} = \gamma_0\beta e^{-i\vec{k}\vec{\tau}_2}$; $H_{B_2'A_1} = \gamma_0\beta e^{-i\vec{k}\vec{\tau}_3}$.

$$\epsilon C_{A_1'} + H_{A_1'B_1'}C_{B_1'} + H_{A_1'B_2}C_{B_2} + H_{A_1'B_2'}C_{B_2'} + \sum_\lambda W_{A_1',\lambda}C_\lambda = EC_{A_1'}, \quad (85)$$

where $H_{A'_1B'_1} = \gamma_0 e^{i\vec{k}\vec{\tau}_1}$; $H_{A'_1B_2} = \gamma_0\beta e^{i\vec{k}\vec{\tau}_3}$; $H_{A'_1B'_2} = \gamma_0\beta e^{i\vec{k}\vec{\tau}_2}$. Here $\lambda$ denotes the atoms of the unitary cell localized on the inner shell. Now we write down the equations for the inner shell in the case of zigzag nanotubes.

$$\tilde{\epsilon}C_A + H_{AB}C_B + H_{AB'}C_{B'} + \sum_\lambda W_{A,\lambda}C_\lambda = EC_A, \quad (86)$$

where $H_{AB} = \gamma_0 e^{i\vec{k}\vec{\tau}_1}$; $H_{AB'} = \gamma_0\widetilde{\beta}(e^{i\vec{k}\vec{\tau}_2} + e^{i\vec{k}\vec{\tau}_3})$.

$$\tilde{\epsilon}C_B + H_{BA}C_A + H_{BA'}C_{A'} + \sum_\lambda W_{B,\lambda}C_\lambda = EC_B, \quad (87)$$

where $H_{BA} = \gamma_0 e^{-i\vec{k}\vec{\tau}_1}$; $H_{BA'} = \gamma_0\widetilde{\beta}(e^{-i\vec{k}\vec{\tau}_2} + e^{-i\vec{k}\vec{\tau}_3})$.

$$\tilde{\epsilon}C_{A'} + H_{A'B}C_B + H_{A'B'}C_{B'} + \sum_\lambda W_{A',\lambda}C_\lambda = EC_{A'}, \quad (88)$$

where $H_{A'B'} = \gamma_0 e^{i\vec{k}\vec{\tau}_1}$; $H_{A'B} = \gamma_0\widetilde{\beta}(e^{i\vec{k}\vec{\tau}_2} + e^{i\vec{k}\vec{\tau}_3})$.

$$\tilde{\epsilon}C_{B'} + H_{B'A}C_A + H_{B'A'}C_{A'} + \sum_\lambda W_{B',\lambda}C_\lambda = EC_{B'}, \quad (89)$$

where $H_{B'A'} = \gamma_0 e^{-i\vec{k}\vec{\tau}_1}$; $H_{B'A} = \gamma_0\widetilde{\beta}(e^{-i\vec{k}\vec{\tau}_2} + e^{-i\vec{k}\vec{\tau}_3})$ and $\lambda$ denotes the atoms of the unitary cell localized on the outer shell.

## Appendix B

In a tight-binding approximation for the case of armchair tubules we get the following systems of equations: for the outer shell

$$\epsilon C_{A_1} + H_{A_1B_1}C_{B_1} + H_{A_1B'_2}C_{B'_2} + \sum_\lambda W_{A_1,\lambda}C_\lambda = EC_{A_1}, \quad (90)$$

where $H_{A_1B_1} = \gamma_0\alpha e^{i\vec{k}\vec{\tau}_1}$; $H_{A_1B'_2} = \gamma_0\beta(e^{i\vec{k}\vec{\tau}_2} + e^{i\vec{k}\vec{\tau}_3})$.

$$\epsilon C_{B_1} + H_{B_1A_1}C_{A_1} + H_{B_1A_2}C_{A_2} + \sum_\lambda W_{B_1,\lambda}C_\lambda = EC_{B_1}, \quad (91)$$

where $H_{B_1A_1} = \gamma_0\alpha e^{-i\vec{k}\vec{\tau}_1}$; $H_{B_1A_2} = \gamma_0\beta(e^{-i\vec{k}\vec{\tau}_2} + e^{-i\vec{k}\vec{\tau}_3})$.

$$\epsilon C_{A_2} + H_{A_2B_2}C_{B_2} + H_{A_2B_1}C_{B_1} + \sum_\lambda W_{A_2,\lambda}C_\lambda = EC_{A_2}, \quad (92)$$

where $H_{A_2B_2} = \gamma_0\alpha e^{i\vec{k}\vec{\tau}_1}$; $H_{A_2B_1} = \gamma_0\beta(e^{i\vec{k}\vec{\tau}_2} + e^{i\vec{k}\vec{\tau}_3})$.

$$\epsilon C_{B_2} + H_{B_2A'_1}C_{A'_1} + H_{B_2A_2}C_{A_2} + \sum_\lambda W_{B_2,\lambda}C_\lambda = EC_{B_2}, \quad (93)$$

where $H_{B_2A_2} = \gamma_0\alpha e^{-i\vec{k}\vec{\tau}_1}$; $H_{B_2A'_1} = \gamma_0\beta(e^{-i\vec{k}\vec{\tau}_2} + e^{-i\vec{k}\vec{\tau}_3})$.

$$\epsilon C_{A'_1} + H_{A'_1B_2}C_{B_2} + H_{A'_1B'_1}C_{B'_1} + \sum_\lambda W_{A'_1,\lambda}C_\lambda = EC_{A'_1}, \quad (94)$$

where $H_{A'_1B'_1} = \gamma_0\alpha e^{i\vec{k}\vec{\tau}_1}$; $H_{A'_1B_2} = \gamma_0\beta(e^{i\vec{k}\vec{\tau}_2} + e^{i\vec{k}\vec{\tau}_3})$.

$$\epsilon C_{B'_1} + H_{B'_1A'_1}C_{A'_1} + H_{B'_1A'_2}C_{A'_2} + \sum_\lambda W_{B'_1,\lambda}C_\lambda = EC_{B'_1}, \quad (95)$$

where $H_{B'_1A'_1} = \gamma_0\alpha e^{-i\vec{k}\vec{\tau}_1}$; $H_{B'_1A'_2} = \gamma_0\beta(e^{-i\vec{k}\vec{\tau}_2} + e^{-i\vec{k}\vec{\tau}_3})$.

$$\epsilon C_{A'_2} + H_{A'_2B'_1}C_{B'_1} + H_{A'_2B'_2}C_{B'_2} + \sum_\lambda W_{B'_2,\lambda}C_\lambda = EC_{B'_2}, \quad (96)$$

where $H_{A'_2B'_2} = \gamma_0\alpha e^{i\vec{k}\vec{\tau}_1}$; $H_{A'_2B'_1} = \gamma_0\beta(e^{i\vec{k}\vec{\tau}_2} + e^{i\vec{k}\vec{\tau}_3})$.

$$\epsilon C_{B'_2} + H_{B'_2A_1}C_{A_1} + H_{B'_2A'_2}C_{A'_2} + \sum_\lambda W_{B'_2,\lambda}C_\lambda = EC_{B'_2}, \quad (97)$$

where $H_{B'_2A'_2} = \gamma_0\alpha e^{-i\vec{k}\vec{\tau}_1}$; $H_{B'_2A_1} = \gamma_0\beta(e^{-i\vec{k}\vec{\tau}_2} + e^{-i\vec{k}\vec{\tau}_3})$. Here $\lambda$ denotes the atoms of the unitary cell localized on the inner shell. The equations for the inner shell can be expressed in the form:

$$\tilde{\epsilon}C_A + H_{AB'}C_{B'} + H_{AB}C_B + \sum_\lambda W_{A,\lambda}C_\lambda = EC_A, \quad (98)$$

where $H_{AB} = \gamma_0\widetilde{\alpha}e^{i\vec{k}\vec{\tau}_1}$; $H_{AB'} = \gamma_0\widetilde{\beta}(e^{i\vec{k}\vec{\tau}_2} + e^{i\vec{k}\vec{\tau}_3})$.

$$\tilde{\epsilon}C_B + H_{BA}C_A + H_{BA'}C_{A'} + \sum_\lambda W_{B,\lambda}C_\lambda = EC_B, \quad (99)$$

where $H_{BA} = \gamma_0\widetilde{\alpha}e^{-i\vec{k}\vec{\tau}_1}$; $H_{BA'} = \gamma_0\widetilde{\beta}(e^{-i\vec{k}\vec{\tau}_2} + e^{-i\vec{k}\vec{\tau}_3})$.

$$\tilde{\epsilon}C_{A'} + H_{A'B}C_B + H_{A'B'}C_{B'} + \sum_\lambda W_{A',\lambda}C_\lambda = EC_{A'}, \quad (100)$$

where $H_{A'B'} = \gamma_0\widetilde{\alpha}e^{i\vec{k}\vec{\tau}_1}$; $H_{A'B} = \gamma_0\widetilde{\beta}(e^{i\vec{k}\vec{\tau}_2} + e^{i\vec{k}\vec{\tau}_3})$.

$$\tilde{\epsilon}C_{B'} + H_{B'A}C_A + H_{B'A'}C_{A'} + \sum_\lambda W_{B',\lambda}C_\lambda = EC_{B'}, \quad (101)$$

where $H_{BA'} = \gamma_0\widetilde{\alpha}e^{-i\vec{k}\vec{\tau}_1}$; $H_{B'A} = \gamma_0\widetilde{\beta}(e^{-i\vec{k}\vec{\tau}_2} + e^{-i\vec{k}\vec{\tau}_3})$. Here $\lambda$ denotes the atoms of the unitary cell localized on the outer shell.

## References


1. T. Sugai, H. Yoshida, T. Shimada, T. Okazaki, H. Shinohara, Nano Lett. **3**, 769 (2003)
2. Z. Zhou et al., Carbon **41**, 337 (2003)
3. Y. Kwon, D. Tomanek, Phys. Rev. B **58**, R16001 (1998)
4. Y. Miyamoto, S. Saito, D. Tomanek, Phys. Rev. B **65**, 041402(R) (2001)
5. S. Okada, A. Oshiyama, Phys. Rev. Lett. **91**, 216801 (2003)
6. V. Zólyomi, J. Koltai, Á. Rusznyák, J. Kürti, Á. Gali, F. Simon, H. Kuzmany, Á. Szabados, P.R. Surján, Phys. Rev. B **77**, 245403 (2008)

7. V. Zólyomi, Á. Rusznyák, J. Kürti, Á. Gali, F. Simon, H. Kuzmany, Á. Szabados, P.R. Surján, Phys. Stat. Sol. (b) **243**, 3476 (2006)
8. Y.H. Ho, C.P. Chang, F.L. Shyu, R.B. Chen, S.C. Chen, M.F. Lin, Carbon **42**, 3159 (2004)
9. R. Saito, G. Dresselhaus, M.S. Dresselhaus, J. Appl. Phys. **73**, 494 (1993)
10. Y.H. Ho, G.W. Ho, S.J. Wu, M.F. Lin, J. Vac. Sci. Technol. B **24**, 1098 (2006)
11. P. Lambin, V. Meunier, A. Rubio, Phys. Rev. B **62**, 5129 (2000)
12. M. Pudlak, R. Pincak, V.A. Osipov, Phys. Rev. B **74**, 235435 (2006)
13. R. Pincak, M. Pudlak, *Progress in Fullerene Research* (Milton Lang, Nova Science Publisher, 2007), Chap. 7, pp. 235–268, ISBN 1-60021-841-5
14. F. Triozon, S. Roche, A. Rubio, D. Mayou, Phys. Rev. B **69**, 121410(R) (2004)
15. C.H. Lee et al., J. Phys.: Condens. Matter **20**, 075213 (2008)
16. Y.J. Kang, K.J. Chang, Y.H. Kim, Phys. Rev. B **76**, 205441 (2007)
17. J.-C. Charlier, X. Blase, S. Roche, Rev. Mod. Phys. **79**, 677 (2007)
18. R. Saito, M. Fujita, G. Dresselhaus, M.S. Dresselhaus, Phys. Rev. B **46**, 1804 (1992)
19. T. Frankel, *The Geometry of Physics* (Cambridge University Press, Cambridge, 1999)
20. A. Kleiner, S. Eggert, Phys. Rev. B **64**, 113402 (2001)
21. W.M. Lomer, Proc. Roy. Soc. A **227**, 330 (1955)
22. C.L. Kane, E.J. Mele, Phys. Rev. Lett. **78**, 1932 (1997)
23. A.G.S. Filho et al., Nano Letters **7**, 2383 (2007)
24. B. Shan, K. Cho, Phys. Rev. B **73**, 081401(R) (2006)
25. P.N. Dyachkov, D.V. Makaev, Phys. Rev. B **74**, 155 (2006)
26. C.D. Spataru, S. Ismail-Beigi, L.X. Benedict, S.G. Louie, Phys. Rev. Lett. **92**, 077402 (2004)
27. W. Song, M. Ni, J. Lu, Z. Gao, S. Nagase, D. Yu, H. Ye, X. Zhang, Chem. Phys. Lett. **414**, 429 (2005)
28. V. Zólyomi, J. Kürti, Phys. Rev. B **70**, 085403 (2004)
29. S.W.D. Bailey, I. Amanatidis, C.J. Lambert, Phys. Rev. Lett. **100**, 256802 (2008)